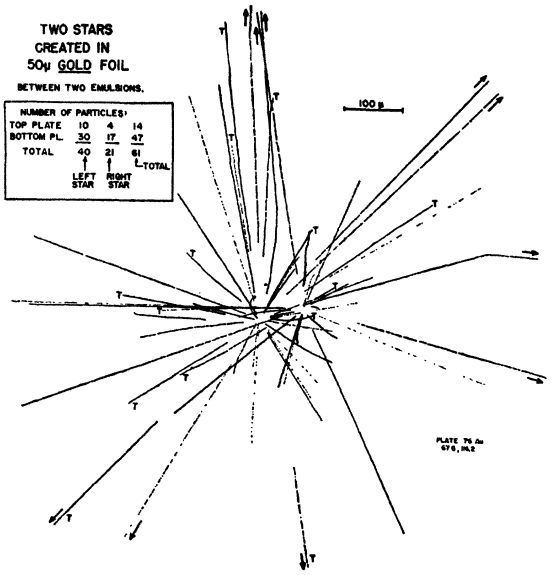

FIG. 1. Microprojection of tracks from two neighboring stars caused by the disintegration of gold nuclei. All the tracks can be seen to radiate from two points between the emulsions; the central portion of each track, representing the portion of the trajectory within the foil, is not observable. Tracks marked "T" were in the top plate, others in the bottom plate; arrows indicate tracks continuing beyond this field of view in the emulsion.

found that a new metal foil, even under moderate pressure, will not lie completely flat during exposure. It was found necessary to heat each foil to its annealing temperature to render it malleable, and then subject it to high pressure between two very flat steel surfaces. Finally the flattened foil is placed between 10μ sheets of cellulose acetate (or better, coated with a very thin layer of plastic) to prevent the interaction of the metal atoms with those of the emulsion. Clamped between pairs of nuclear plates, foils of Au, Pt, Ni, Cu, Sn, and Al were flown together in a flight of 6 hr. at 93,000 ft.[5]

After removal of the foils and development of the emulsions, the corresponding plates were placed face-to-face, the original alignment being reconstructed by x-ray dots[6] at the ends of the plates and by exact alignment of through tracks, and the edges were cemented, so that the pair of emulsions could be scanned together and observed with a magnification of 450×. Figure 1 is a microprojection of tracks from the disintegration of two gold nuclei which happened to be quite near each other. The weight and area of each foil were accurately measured, so that it was possible to calculate from the number of stars observed the cross section for star production per target nucleus. The correction for tracks missed outside the field of view was computed after determining the original emulsion separation by geometrical consideration of through tracks; a small correction for star tracks which never leave the foil must also be applied. Figure 2 shows values found for relative cross sections *per target nucleus* for the production of stars of various sizes in four materials. The data on very small stars (3, 4, and even 5 prongs) in the foils must be considered less reliable, because of the possibility that tracks, from a 4-prong star, for instance, could be so oriented in the two emulsions that the scanner might overlook their association with a common origin. The values for the emulsion stars are greater than anticipated, though the variety of elements present and uncertainty as to density and shrinkage factor make an exact interpretation difficult. Analysis of the complete data indicates a maximum at about 8 prongs per star for Au, and 6 for Sn, whereas for Cu and emulsion it occurs for smaller values. As an insert in Fig. 1 the integral cross section for stars of more than 4, 8, 6, and 10 prongs have been plotted on a log-log graph against the atomic weight, A, of the target nucleus. Approximate linearity indicates a dependence

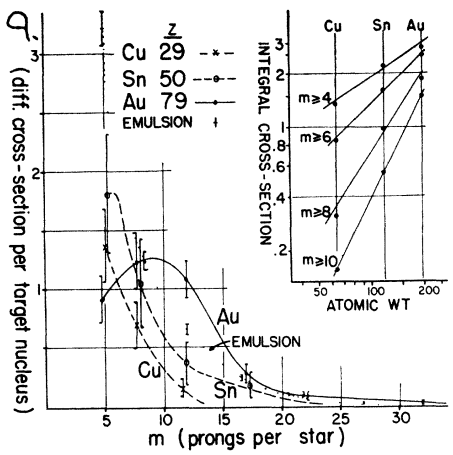

FIG. 2. Differential cross section (number of stars of m prongs observed per target nucleus $\times 10^{-21}$) *vs.* number of prongs (m) for four target materials. Insert at upper right shows a log-log plot of integral cross section (for stars of more than 4, 6, 8, and 10 prongs) *vs.* the atomic weight of the target foil.

of the form $\sigma_r = kA^s$, where for values of r (the minimum number of prongs considered) of 10, 8, 6, and 4, the corresponding values of the exponent, s, are 2.0, 1.5, 1.0, and 0.7. Estimating the extrapolation to include stars of 2 or 3 prongs, the total cross section for stars of all sizes is quite close to an $A^{\frac{2}{3}}$ law. This data refers to all observed star tracks and therefore includes, for each star, particles from both initial nucleon-nucleon collision processes and from subsequent "evaporation." A separate analysis of the groups of energetic particles ("meson showers"), their angular distribution and cross section as a function of the atomic weight, together with completion of the data on other metal foils, is in progress.

* This work has been aided by a Cottrell Grant from the Research Corporation.

† Now at Ohio State University, Columbus, Ohio.

[1] Camerini, Fowler, Lock, and Muirhead, Phil. Mag. **41**, 413 (1950).
[2] D. H. Perkins, *Cosmic Radiation* (Butterworth's Ltd., London, 1949).
[3] J. B. Harding, Nature **163**, 440 (1949).

[4] As a check on the present experiment, we are exposing such a suspension of Pb powder prepared by E. Hones of Duke University.

[5] Arranged through the kindness of the ONR and the General Mills Company.

[6] I. Barbour, Phys. Rev. **78**, 518 (1950).

Mesons Produced in Proton-Proton Collisions*

VINCENT Z. PETERSON
Radiation Laboratory, University of California, Berkeley, California
June 5, 1950

A FUNDAMENTAL problem in the study of mesons is that of their production in the collisions of protons with free protons, since the analysis is unhindered by considerations of the internal dynamics of complexed nuclei. Such an experiment can be performed by using a subtraction technique[1] employing C and CH_2, or a pure hydrogen target can be used to study the production directly. We have chosen to construct a liquid hydrogen target and have studied the meson energy distribution at various angles with respect to an incident beam of 345-Mev protons from the Berkeley 184-inch cyclotron.

Since the threshold for meson production in proton-proton collisions is very high (292 Mev in the laboratory system), the maximum kinetic energy available to the meson in the center-of-mass system is only about 25 Mev (for 345-Mev protons incident). Such a meson will have a velocity only slightly greater than the center-of-mass velocity, and hence the meson flux may be expected to be emitted in a predominantly forward direction in the laboratory system. Furthermore, the upper limit of meson energy decreases rapidly with angle, from 74 Mev at 0° to 7 Mev at 90°.

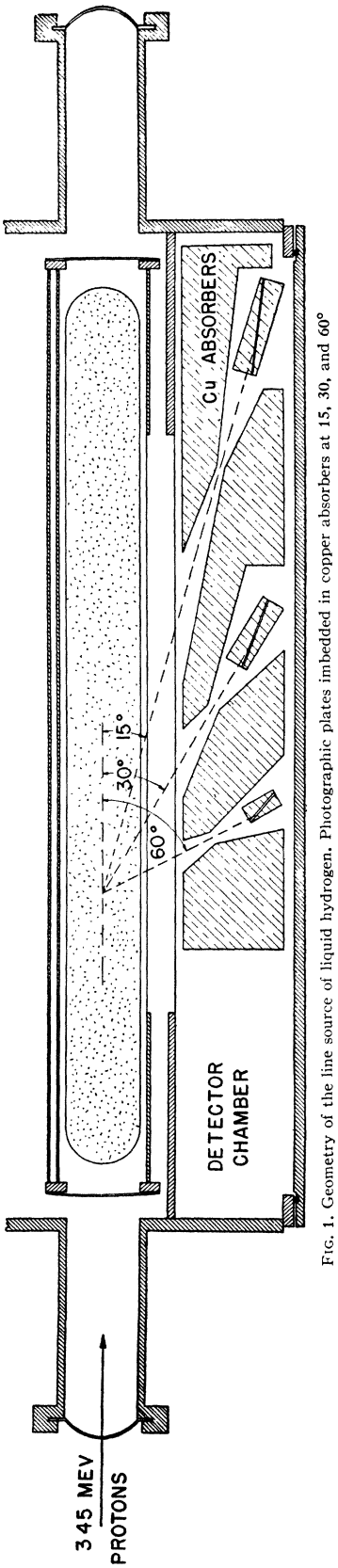

FIG. 1. Geometry of the line source of liquid hydrogen. Photographic plates imbedded in copper absorbers at 15, 30, and 60°

Consequently we have looked at 15 and 30° to the incident beam; the data obtained to date at 30° are reported here.

Figure 1 shows the geometry of the earlier experiments in which a line source of liquid hydrogen was used to eliminate end-window effects. Copper collimators serve to shield the photographic plate detectors from excessive background and also serve to define the observation angle and effective target thickness. Ilford C-2 100μ plates imbedded in copper absorbers at an angle to the meson flux sample the volume density of mesons stopping at various ranges in the copper. In this manner a complete energy spectrum can be obtained in one plate, eliminating many relative errors possible in taking energy points separately. The incident proton beam passes through an argon ion chamber before strking the target, so that absolute values of the differential cross section may be determined.

Figure 2 shows the energy spectrum of positive mesons at 30°, based on 115 π–μ-decays observed in one plate exposed using the line source gometry. The most striking feature of this distribution, apparent despite poor statistics, is the concentration of mesons near the upper energy limit. This sharp peak is not predicted by any of the usual meson theories[2] if one assumes that the final proton and neutron do not interact (Born approximation). However, as was first pointed out by Barkas[3] and by Chew,[4] it is not only possible but also likely that the final nucleons will either

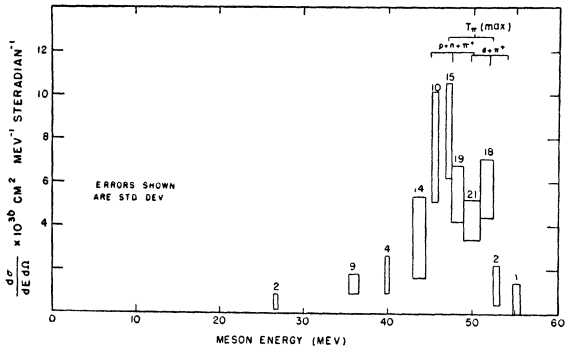

FIG. 2. Energy spectrum of positive π-mesons from 335-Mev protons on liquid hydrogen. Observation angle 30°±3°.

interact strongly or may even unite to form a real deuteron. In the latter case the reaction becomes a two-body problem, and one would expect a "line" of mesons of a single energy situated about 4 Mev (at 30° observation angle) beyond the continuous spectrum. It is not possible to confirm or deny the existence of such a line on the basis of the data of Fig. 2, owing to poor statistics and insufficient energy resolution. However, the calculated limits and line positions are shown for the range of angles included.

Since the exclusion principle limits the possible states of the initial proton-proton system, proof of the existence of deuterons in this reaction would impose definite restrictions on the type of meson-nucleon interactions which could be assumed. Therefore, it is of interest go try to improve both statistics and energy resolution in an effort to resolve the line, if it exists, from the continuous distribution. The magnitude of the peak cross section and the lack of negative mesons in the line-source experiments have encouraged us to use a thin-walled (0.002 in.) aluminum cylinder of 1½-in. diameter as a "point" source of liquid hydrogen in order to improve the angular resolution. In addition the use of a bending magnet to sort the positive mesons from elastically scattered protons has improved the meson-to-background ratio in the plates by a factor of about 500, with subsequent improved counting rate. Recent data based on 315 π–μ-decays obtained in this manner confirm the shape of the peak shown in Fig. 1 but still give no definite indication of fine structure. The estimated energy resolution for this run, however, was only about ±4 Mev. Further improvements in the energy resolution of the detection arrangement are being made. The best resolution will be determined by the energy spread of the

incident proton beam, which is estimated to have a total spread of less than 4 Mev.

Miss Dora Sherman and Mr. Edwin Iloff have assisted in scanning the plates.

* This work was sponsored by the AEC.

[1] Cartwright, Richman, Whitehead, and Wilcox, Phys. Rev. **78**, 823 (1950).
[2] K. Brueckner (private communication).
[3] W. Barkas, Phys. Rev. **75**, 1109 (1949).
[4] G. Chew (private communication).

The Beta-Spectrum of Sn^{125}

RAYMOND W. HAYWARD
Department of Physics, University of California, Berkeley, California
May 29, 1950

THE beta-spectrum of the 9.9-day tin activity has been examined in a magnetic lens spectrometer similar to the one described by Siegbahn.[1]

Ketelle, Nelson, and Boyd[2] identified this tin activity as Sn^{125} by irradiating tin samples electromagnetically enriched in Sn^{124} with a high flux of slow neutrons. They were able to milk chemically the 2.7-yr. Sb^{125} activity from the activated tin sample on successive occasions.

A sample of the 9.9-day tin made by fission of thorium by deuterons and chemically separated with 50μg of carrier was furnished by Dr. A. S. Newton. A source was prepared by mounting the sample on a Nylon film supported by a Lucite ring so that the mass of the source was about 0.4 mg/cm^2. A beta-spectrum was obtained and a Fermi plot of the data is shown in Fig. 1. Forgetting for the moment the low energy component, there is the characteristic non-linearity associated with the type of forbidden spectrum in which a spin change of two units and a parity change occur in the transition. In this type of transition it is theoretically appropriate to modify the conventional Fermi plot by dividing the ordinate by a factor $(p^2+q^2)^{\frac{1}{2}}$ where p and q are the momenta of the electron and the neutrino, respectively. When this is done, we obtain the modified Fermi plot shown in Fig. 2 where the linearity indicates the correctness in assuming the interaction to be of the first-forbidden type. The end-point energy from this modified Fermi plot is 2.37±0.02 Mev which is slightly higher than that obtained by Ketelle *et al.* The $f\tau_{\frac{1}{2}}$-value of 3.7×10^8 is in experimental agreement with the other known beta-spectra exhibiting this type of forbidden shape.[3]

The low energy beta-component accounts for about five percent of the total intensity and has an upper energy limit of 0.40±0.01 Mev. From the preceding facts the presence of a gamma-ray of about 2 Mev energy and five percent intensity would be suspected. Efforts to find this gamma-ray by observation of the Compton

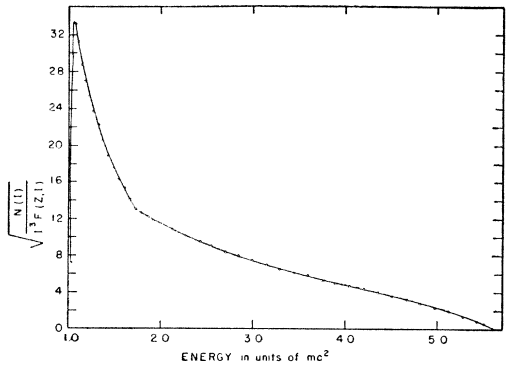

FIG. 1. A conventional Fermi plot of the Sn^{125} beta-spectrum in which only the density of final states for the beta-particle and the neutrino and the perturbation by the Coulomb field of the nucleus on the beta-particle are taken into account.

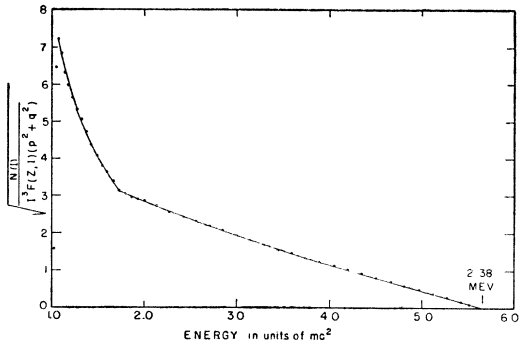

FIG. 2. A modified Fermi plot of the Sn^{125} beta-spectrum in which an additional factor $(p^2+q^2)^{\frac{1}{2}}$ is included, taking into account the dependence of the nuclear matrix elements on the momenta of the beta-particle and the neutrino.

electrons from a copper radiator surrounding a source of Sn^{125} in the spectrometer proved negative, but this could have been due to insufficient activity and the low branching ratio. However, absorption measurements in lead by Newton and McDonell[4] indicate the possible presence of a gamma-ray of about 1.5 Mev which could be the 2-Mev gamma-ray since absorption measurements in this energy range are inherently inaccurate when the intensity is low.

[1] K. Siegbahn, Phil. Mag. **37**, 181 (1946).
[2] Ketelle, Nelson, and Boyd, Bul. Phys. Rev. **79**, 242 (1950).
[3] L. M. Langer and H. C. Price, Jr., Phys. Rev. **76**, 641 (1949).
[4] A. S. Newton and W. R. McDonell (unpublished work).

Electronic Mobility in Germanium*

V. A. JOHNSON AND K. LARK-HOROVITZ
Purdue University, Lafayette, Indiana
May 25, 1950

SOME time agao we analyzed the resistivity behavior[1] of a large number of germanium samples, prepared by adding varying amounts of various elements to high purity germanium. We found that it is possible to account for the observed resistivity from near the melting point down to very low temperatures as the sum of a lattice resistivity ρ_L due to scattering of carriers by lattice ions and an impurity resistivity ρ_I due to the Rutherford scattering of carriers by impurity ions.[2] The mobility associated with ρ_L is characteristic of the germanium lattice and so should be the same, at a given temperature, for all N-type germanium samples.

In our original analysis we used the classical expression for the Hall coefficient, $R=-3\pi/(8ne)$, where R is given in cm^3/coulomb, e in coulombs, and the electron density n in cm^{-3}. Hence the mobility was calculated from $b_L=8|R|/(3\pi\rho_L)$. Such computations yielded a room temperature electron mobility of 1450±300 cm^2/volt-sec. The samples in this group were polycrystalline and of low resistivity material (0.005 to 0.5 ohm-cm). More recently, measurements[3] have been made on samples of very high purity, usually single crystals. Analysis of the data for such samples usually has led to mobility values far higher than those previously obtained. In addition, Pearson, Haynes, and Shockley[4] have found that the mobility measured from drift velocities is constant, the same from sample to sample, but having a value considerably higher than that calculated by the use of $b=8|R|/(3\pi\rho)$.

In the hope of explaining these mobility discrepancies we have re-examined[5] the classical Hall coefficient expression and found that the numerical coefficient should be replaced by a variable quantity whose value is dependent upon the fraction of the total resistivity due to impurity scattering. This modification arises because the classical expression is based on the assumption that the mean free path of a conduction electron is independent of its kinetic energy; such is the case for lattice scattering except at very